Journal of Macromolecular Science, Part A
Publication details, including instructions for authors and subscription information:
http://www.informaworld.com/smpp/title~content=t713597274

Thermal Effect of Phosphate Salt Additives on Poly(L-Lactic Acid) and the Coordination Structure

Akihiro Ito[a]; Shigeo Matsushita[a]; Koichi Kondo[a]
[a] Department of Applied Chemistry, Faculty of Science and Engineering, Ritsumeikan University, Kusatsu, Shiga, Japan

To cite this Article Ito, Akihiro , Matsushita, Shigeo and Kondo, Koichi(2005) 'Thermal Effect of Phosphate Salt Additives on Poly(L-Lactic Acid) and the Coordination Structure', Journal of Macromolecular Science, Part A, 42: 12, 1715 — 1729
To link to this Article: DOI: 10.1080/10601320500247212
URL: http://dx.doi.org/10.1080/10601320500247212

Journal of Macromolecular Science®, Part A: Pure and Applied Chemistry, 42:1715–1729, 2005

ISSN 1060-1325 print/1520-5738 online
DOI: 10.1080/10601320500247212

Thermal Effect of Phosphate Salt Additives on Poly(L-Lactic Acid) and the Coordination Structure

AKIHIRO ITO, SHIGEO MATSUSHITA, AND KOICHI KONDO

Department of Applied Chemistry, Faculty of Science and Engineering, Ritsumeikan University, Kusatsu, Shiga, Japan

Poly(L-lactic acid) (PLLA) was mixed with a few weight percent of magnesium or calcium hydrogen phosphate to improve the thermal property. Calcium hydrogen phosphate as an additive to PLLA was found to be more effective in increasing the glass transition point (T_g) than magnesium hydrogen phosphate, which was investigated by the differential scanning calorimetry (DSC) and thermogravimetric analysis (TGA). Studies on the coordination structure for the polymer complex (ca-(plla)) confirmed by infrared (IR) spectroscopy and extended X-ray absorption fine structure (EXAFS) indicated that calcium ion radius would be suitable for the coordination with carbonyl groups of polymer chains.

Keywords poly(L-lactic acid), calcium hydrogen phosphate, magnesium hydrogen phosphate, CA-(plla) polymer complex, coordination, extended X-ray absorption fine structure (EXAFS), T_g

Introduction

Poly(L-lactic acid) (PLLA) has attracted much attention due to the biodegradability that is expected for potential use as an environmentally benign plastic. At present, biomedical uses such as implants (1), nuclear oncology (2–3) and orthopedic surgery field (4, 5) are promising. However, PLLA still is not widely used as common plastics due to the low T_g (57°C) and the a lesser amount of impact strength, despite PLLA in T_g which is superior to other biodegradable aliphatic polyesters such as poly(β-hydroxybutyrate), poly(ε-caprolactone) and polybutylene succinate (T_g; 4, −60, and −32°C. respectively) (6). Among a variety of trials to improve the thermal property which have been conducted so far (7–14), the addition of inorganic substances to polymers would be one of the feasible methods to increase T_g because the polymer chains can be fixed through crosslinkings or the coordination with metal ions on carbonyl groups of PLLA (13–17). As for the present investigation of the PLLA-metal complex, the coordination features have been discussed only by a few workers (18–21), and the precise coordination structure, such as the coordination number and the coordination length has not been extensively investigated. Therefore, the PLLA metal complex should be resolved in terms of the coordination structures along with the thermal property.

Received August 2004; Accepted March 2005.
Address correspondence to Koichi Kondo, Department of Applied Chemistry, Faculty of Science and Engineering, Ritsumeikan University, 1-1-1 Nojihigashi, Kusatsu, Shiga 525-8577, Japan. E-mail: koichi@se.ritsumei.ac.jp

This report describes the coordination behavior and thermal effect of magnesium or calcium hydrogen phosphate additives on PLLA. Uses of magnesium or calcium hydrogen phosphate as additives to polymer are reasonable due to the cheap cost and the non-toxicity as appeared in other polymer cases (15–17), as well as the enhancement of biodegradability of PLLA by the addition of calcium salts (13, 16). The coordination structure of PLLA-metal complex was investigated by infrared (IR) spectroscopy and extended X-ray absorption fine structure (EXAFS), together with the thermal properties of PLLA-metal complex studied by differential scanning calorimetry (DSC) and thermogravimetric analysis (TGA).

Experimental

Materials

PLLA was prepared from the solid-state postpolymerization of L-lactide (Tokyo Kasei, Tokyo) using stannous 2-ethylhexanoate ($Sn(Oct)_2$, Nacalai tesque, Kyoto) as a catalyst at 200°C for 2 min followed by 140°C for 20 h (22). Crude polymer was purified by a reprecipitation of the chloroform solution into methanol. The polymer thus obtained was dried under reduced pressure. The number-average molecular weight (M_n) of PLLA was determined by gel permeation chromatography (GPC) (a Shimadzu LC-10AD pump equipped with a Shimadzu RID-10A RI detector, a Shimadzu C-R7A chromatopac data processor, and eluted with tetrahydrofuran (THF, HPLC grade, Nacalai tesque) at 25°C on Toso TSKgel Super AW4000, AW3000, and AW2500) to yield 2.61×10^5 (calibrated with polyethylene oxide standard) (M_w/M_n:1.06).

Magnesium hydrogen phosphate trihydrate and calcium hydrogen phosphate dihydrate are commercially available, and used after 1 week dryness under reduced pressure. The hydration number determined by the Karl-Fischer method to the DMSO solution was 0.4 for magnesium salt and 0.7 for calcium salt, respectively.

Sample Preparation

A given amount of phosphate salt was added to PLLA and mixed thoroughly in a mortar and pestle. Powder sample was mixed with dichloromethane to the 50 wt% solution. After evaporation of the solvent on a hot plate, the paste was melted at 190°C, and annealed at 120°C for 1 h to form the film or tip that was served for X-ray analyses. The Mg or $CaHPO_4$-PLLA complex was dehydrated completely during a sample processing, and served for DSC and thermogravimetric analysis (TGA).

IR Measurements

IR spectra were taken by a Shimadzu FT-IR 8600 in the range of 400 to 4600 cm^{-1}, with 1.0 cm^{-1} resolution and 40 scan times. The film for measurements was made by casting the dichloromethane phosphate-PLLA solution (0.5 wt%) on a NaCl plate, subsequently evaporating of the solvent, melting at 190°C for 1 h, and annealing at 120°C for 1 h. IR spectra for phosphate salts were measured by the KBr method.

EXAFS Study

The X-ray absorption spectra were measured at the K-edge of calcium (4038 eV) in transmission mode at the Synchrotron radiation (SR) center BL-4 (Ritsumeikan

University, Japan), using a Ge[220] double crystal monochromator in an ion chamber as a detector filled with N_2 (85%)–Ar (15%) mixing gas. The $CaHPO_4$-PLLA film sandwiched with two polyethyleneterephthalate films (thickness; 0.1 mm) was served for EXAFS.

DSC Analyses

Thermal properties of PLLA-metal complexes (3 mg in an aluminum pan) were determined by DSC (a Shimadzu DSC-50 on TA-50WS thermal analyzer) at a heating rate of 10°C min^{-1}, cooling rate of 10°C min^{-1} under nitrogen atmosphere.

TGA Measurement

The decomposition point (the temperature of 10% wt loss for PLLA) was determined by TGA (a Shimadzu TGA-50 on TA-50WS thermal analyzer), heating at 10°C min^{-1} to 400°C under a nitrogen atmosphere.

Results and Discussion

IR Measurements

The coordination behavior of magnesium or calcium hydrogen phosphate salt was confirmed by IR spectra which were varied with the phosphate salt concentration. A wide range scanning of spectra (4600 to 400 cm^{-1}) was difficult to assign each band clearly, but the enlargement of 1850 to 1600 cm^{-1} region made a significant difference in carbonyl stretching vibration band (around 1757 cm^{-1}) (Figures 1–2). Obviously, spectra of $CaHPO_4$-PLLA complexes (1.43 mmol g^{-1}) were different from those of $MgHPO_4$-PLLA complexes (1.54 mmol g^{-1}), which almost overlapped with the spectrum of PLLA itself (Figure 3).

EXAFS Study (23)

When the C═O stretching vibration band of the $CaHPO_4$-PLLA complex (1.43 mmol g^{-1}) was fitted with the non-linear least-square method using the summation function of Gaussian-Lorenzian (Figure 4), the fitting results included the Gaussian component of 0.4444 (standard deviation; 0.0258), error square sum of 0.0521, and *R*-factor of 0.0198. In Figure 4, the peaks were at least separated into four bands of 1778, 1757, 1748, and 1718 cm^{-1} (dotted-dash line) that could be assigned to four types of coordinations related to free carbonyl (in a coordinated polymer chain), free carbonyl (in a bare polymer chain), interacted carbonyl (in a monodentate polymer chain), and interacted carbonyl (in a bidentate polymer chain), respectively.

A $MgHPO_4$-PLLA complex fine powder was not dissolved by X-ray absorption spectra because the K-edge of magnesium was too low (1303 eV) in the energy to separate the photoelectron of absorption atoms from that of other light atoms and auger electrons. As the reference sample for the $CaHPO_4$-PLLA complex, $CaHPO_4 \cdot 2H_2O$ was selected since the crystal structure is known (24, 25). The $k^3\chi(k)$ curves (EXAFS curves) of the $CaHPO_4$-PLLA complex and $CaHPO_4 \cdot 2H_2O$ are shown in Figure 5. The radial structure functions (RSFs) are shown in Figure 6 and were obtained by the

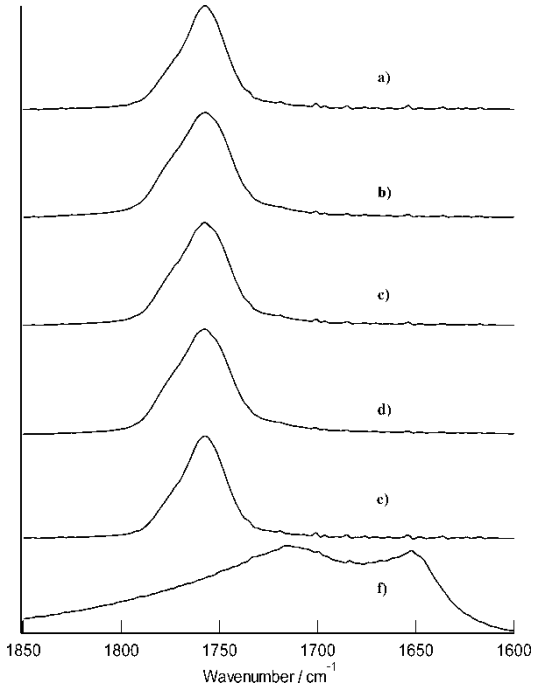

Figure 1. IR spectra around C═O streching vibration band for $MgHPO_4$-PLLA, $[Mg^{2+}]$ = a) 0, b) 0.394, c) 0.784, d) 1.20, e) 1.54 mmol g^{-1}, f) $MgHPO_4$.

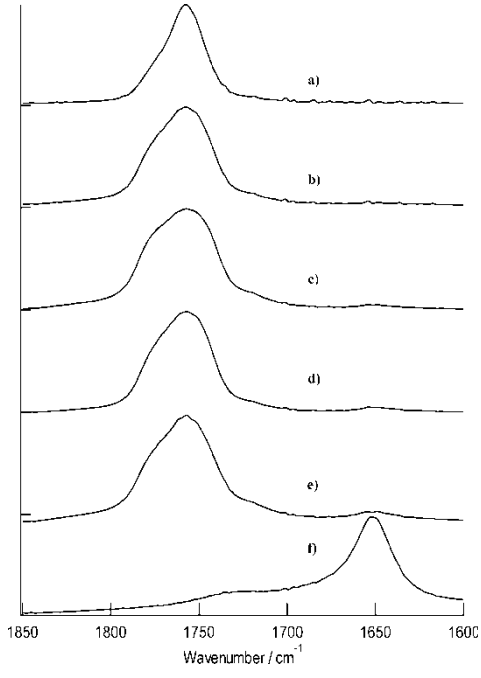

Figure 2. IR spectra around C═O streching vibration band for $CaHPO_4$-PLLA, $[Ca^{2+}]$ = a) 0, b) 0.463, c) 0.951, d) 1.43, e) 1.83 mmol g^{-1}, f) $CaHPO_4$.

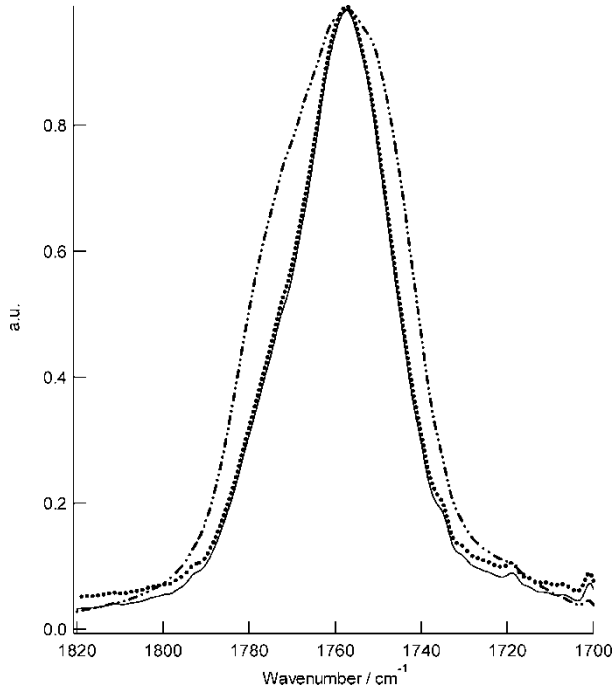

Figure 3. C═O stretching vibration band for PLLA (solid line), $MgHPO_4$-PLLA (dotted line), and $CaHPO_4$-PLLA (dotted-dash line).

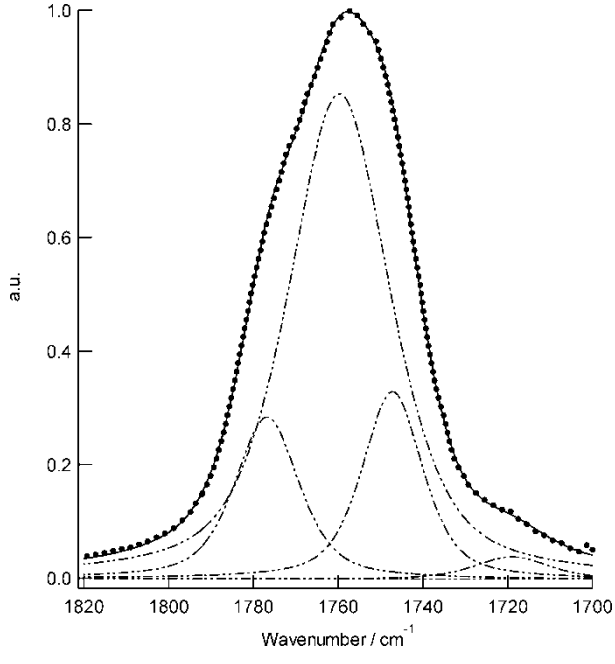

Figure 4. Peak separation of C═O vibration band for $CaHPO_4$-PLLA ($1.43\,mmol\,g^{-1}$), experimental (dotted line), calculated (dotted-dash line), fitting curve (solid line).

following Equation (1).

$$F(r) = \sqrt{\frac{1}{2\pi}} \int_{k_{\min}}^{k_{\max}} k^3 \chi_{\text{obs}}(k) w(k) \cdot \exp(-2ikr) \mathrm{d} \quad \cdots \tag{1}$$

where k is the photoelectron's wave vector, $w(k)$ is the window function, and r is the optical-path. The RSF was not corrected for a phase shift. Fourier filtered $k^3\chi(k)$ curves are shown in Figure 7 (dotted line) that was obtained by back Fourier transformed from the RSF's first peak (around 2 Å). Back Fourier transformation is as follows (Equation 2):

$$k^3 \chi_{\text{filt}}(k) = \sqrt{\frac{1}{2\pi}} \int_{R_{\min}}^{R_{\max}} w(R) F(R) \cdot \exp(2ikR) \mathrm{d}R \quad \cdots \tag{2}$$

The theoretical function of EXAFS function ($\chi_{\text{calc}}(k)$) is:

$$\chi_{\text{calc}}(k) = \sum \left(\frac{n_i}{k r_i^2} \right) \exp\left\{ -2\left(\sigma_i^2 k^2 + \frac{r_i}{\lambda} \right) \right\} f_i(\pi, k) \sin\{2kr_i + \alpha_i(k)\} \quad \cdots \tag{3}$$

where r_i is the length from the absorption atom to ith shell, n_i is the coordination number in ith shell, σ_i is the Debye-Waller factor, $\alpha_i(k)$ is the phase factor of absorbing and scattering atoms, λ is the mean-free-path of photoelectrons, and $f_i(\pi,k)$ is the back

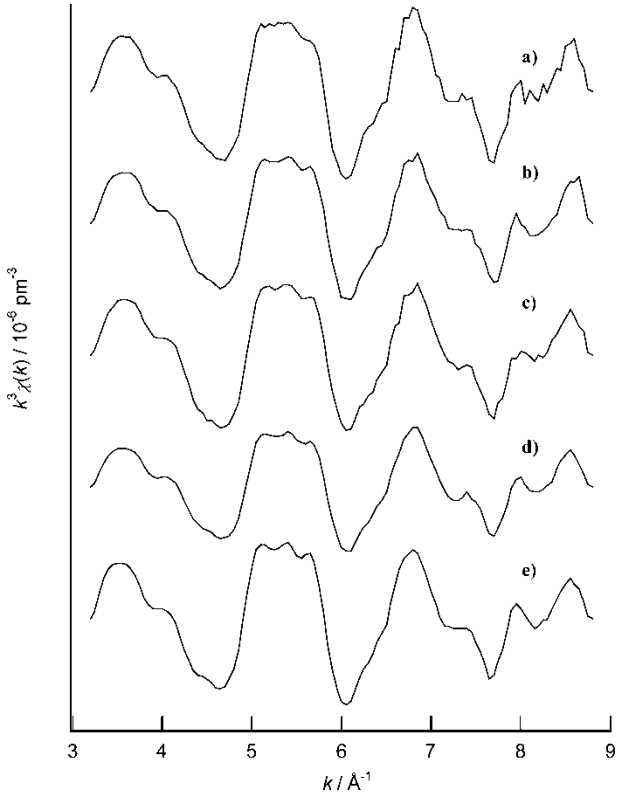

Figure 5. Observed $k^3\chi(k)$ curves for $CaHPO_4$-PLLA, $[Ca^{2+}]$ = a) 0.463, b) 0.951, c) 1.43, d) 1.83 mmol g^{-1}, e) $CaHPO_4 \cdot 2H_2O$.

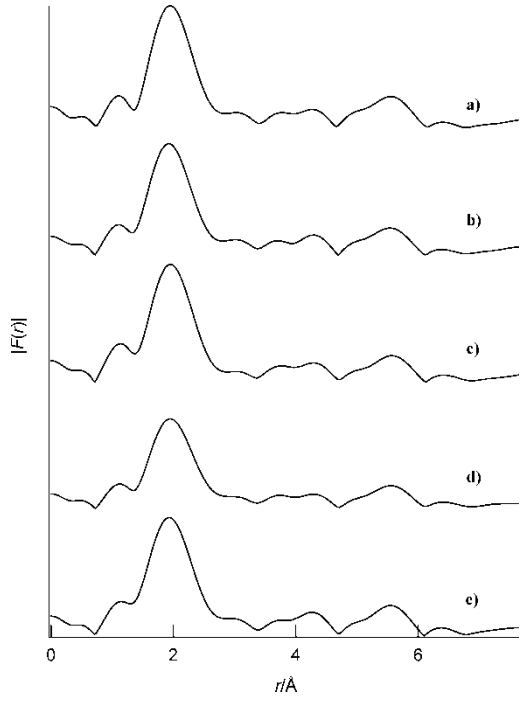

Figure 6. Radial structure functions for $CaHPO_4$-PLLA, $[Ca^{2+}] =$ a) 0.463, b) 0.951, c) 1.43, d) 1.83 mmol g^{-1}, e) $CaHPO_4 \cdot 2H_2O$.

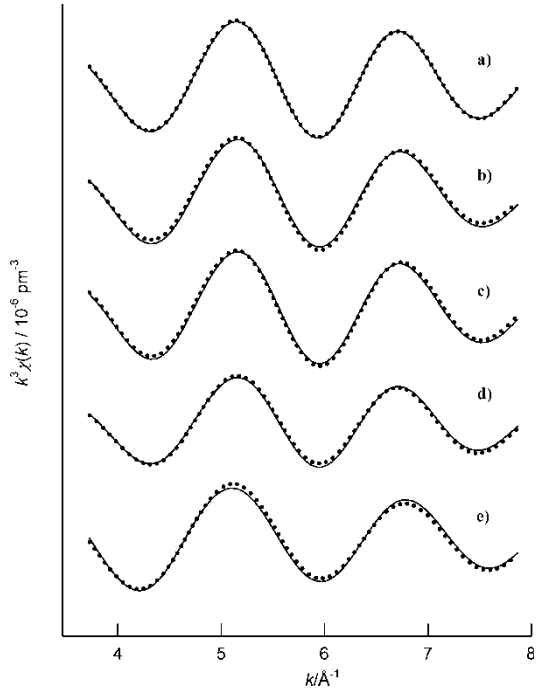

Figure 7. Fourier filtering (dotted line) and calculated (solid line) $k^3\chi(k)$ curves for $CaHPO_4$-PLLA, $[Ca^{2+}] =$ a) 0.463, b) 0.951, c) 1.43, d) 1.83 mmol g^{-1}, e) $CaHPO_4 \cdot 2H_2O$.

scattered amplitude. In this case, $f_i(\pi,k)$ is obtained from the value reported by McKale et al. (26). The $k^3\chi_{filt}(k)$ function was fitted with a $k^3\chi_{calc}(k)$ function using a non-linear least square method (Figure 7, solid line). The fitting results are summarized in Table 1.

The first peak of RSF for $CaHPO_4$-PLLA complex shifted to a longer position compared with that of $CaHPO_4 \cdot 2H_2O$ (Figure 6). Since the coordination length of $CaHPO_4$ anhydrate or $CaHPO_4 \cdot H_2O$ is shorter than that of $CaHPO_4 \cdot 2H_2O$, (24) the peak shift was considered to correspond to $CaHPO_4$-plla (plla as ligand instead of PLLA) complex formation in which the coordination number was estimated to be 6.4 (Figure 7, Table 1). During measurements using a film sample (solid state), hexa- and hepta-coordinated complexes would coexist for the $CaHPO_4$-PLLA complex without the equilibrium between the complexes. The coordination length for Ca-O was estimated to be 242 pm and 298 pm (Table 1). Generally, as the coordination length would be become longer for the bulky ligand, such as a polymer chain coordinated to metals, the longer coordination shell should be assigned to a $Ca\text{-}O_{plla}$, and a smaller one assigned to $Ca\text{-}O_{phosphate}$. Based on these findings, the structural models for $CaHPO_4$-plla complexes are shown in Figure 8. Thus, the structure of $CaHPO_4$-plla complexes would include five types of coordination models: The carbonyl oxygen of PLLA accounts for mono- or di-coordination to calcium ion, as depicted in the mono-plla coordination models with five phosphate oxygens and PLLA oxygen (Figure 8-A), two carbonyl oxygens from the same polymer chain (Figure 8-E), four phosphate oxygens and two PLLA oxygens from one polymer chain (Figure 8-C), and the di-plla coordination models with two PLLA oxygens from the other polymer chain and four (Figure 8-B) or five phosphate oxygens (Figure 8-D). As shown in Figure 6, the plla may be interacted to Ca^{2+} in two differential ways (mono- and bi-dentate). However, the $Ca\text{-}O_{plla}$ length was given with one parameters obtained by EXAFS studies (Table 1) that were averaged on various coordination structures parameters. Therefore, those models would be feasible structures for $CaHPO_4$-plla complexes based on EXAFS and IR results.

Table 1
Structural parameters around the calcium ion in the $CaHPO_4$-PLLA complex

$[Ca^{2+}]$/mmol g^{-1}	N	R/pm	σ/pm
0.463	4.6 (0.1)	242 (1)	4.0 (0.1)
	1.8 (0.1)	298 (1)	4.0 (0.1)
0.951	4.6 (0.2)	241 (1)	5.5 (0.5)
	1.8 (0.1)	297 (1)	5.5 (0.5)
1.43	4.5 (0.2)	241 (1)	4.8 (0.5)
	1.9 (0.1)	298 (1)	4.8 (0.5)
1.83	4.5 (0.2)	242 (1)	7.4 (0.3)
	1.9 (0.1)	294 (1)	7.4 (0.3)
$CaHPO_4$	3[a]	253 (1)	5.2 (0.3)
	4[a]	237 (1)	5.2 (0.3)
	1[a]	278 (1)	7.3 (0.5)

[a]The value was fixed during the least square calculation. Standard deviation of curve fittings is given in parentheses.

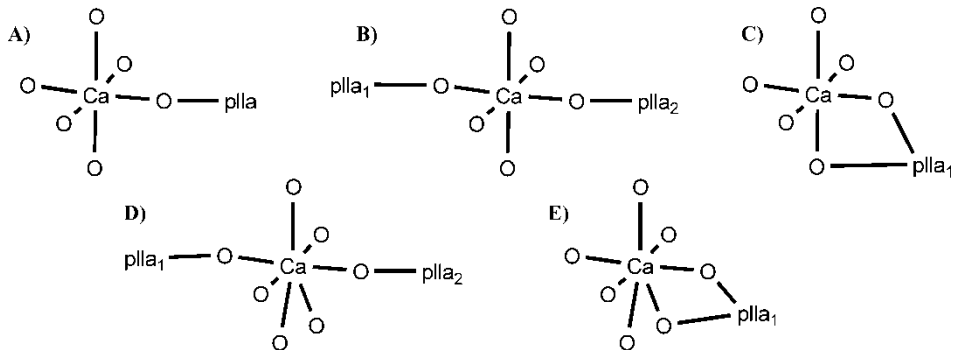

Figure 8. The structural models for $CaHPO_4$-plla complex; hexa-coordinated models (A, B, C) and hepta-coordinated models (D, E). A) five phosphate oxygens with one PLLA oxygen, B) four phosphate oxygens with two PLLA oxygens from two polymer chains, and C) four phosphate oxygens with two PLLA oxygens from one polymer chain, D) five phosphate oxygens with two carbonyl oxygens from each other polymer chain, (E) two carbonyl oxygens from the same polymer chain.

Thermal Properties

The thermal effects of the coordination structure were investigated by DSC and TGA analyses, along with the coordination behavior of phosphate-PLLA complexes confirmed by IR and EXAFS methods. The first and second heating process of DSC curves for each polymer mixed with phosphate salts are shown in Figures 9–12. TGA curves are given in Figures 13–14. In Figures 9–10 and 13–14, the dehydration point appeared around 155°C for $MgHPO_4$-PLLA complex, and 145°C, 190°C for $CaHPO_4$-PLLA complex. From Figure 11–12, thermal properties such as T_g, crystallization point (T_c), crystallization enthalpy (ΔH_c), melting point (T_m), and melting enthalpy (ΔH_m) were determined and summarized in Tables 2 and 3. T_g was estimated at the inflection point from their 2nd heating DSC curves around 55 to 65°C. The decomposition point (10% wt loss point) for PLLA was obtained from Figures 13–14 (Tables 2–3).

T_g was found to increase linearly with increasing $[M^{2+}]$ (M^{2+}: Mg^{2+}, Ca^{2+}) as shown in Figure 15 plotting of T_g against $[M^{2+}]$, whereas T_c tended to decrease when phosphate salt was present. Calcium ion was more efficient than magnesium ion for the increasing of T_g. These results suggest that the strong coordination would be effective for the improvement of thermal properties as observed by IR and EXAFS studies. In addition, the decomposition point for PLLA increased by the addition of phosphate salt to PLLA. Particularly, *T*d of $CaHPO_4$-PLLA complex remarkably was increasing (~80°C) compared with *T*d of $MgHPO_4$-PLLA complex (~20°C). Such an increasing decomposition point for phosphate-PLLA complex was similar to T_g behavior, suggesting that the coordination of metal to PLLA would be also useful for the thermal improvement of PLLA.

Conclusions

Additives such as magnesium or calcium hydrogen phosphate on PLLA were found to increase the interaction of the metal ion with carbonyl groups. IR analyses revealed that there were four types of carbonyl stretching vibrations around 1757 cm^{-1} region for $CaHPO_4$-PLLA complex corresponding to free carbonyl, monodentate polymer, and bidentate polymer. The coordination was confirmed by EXAFS study to give the

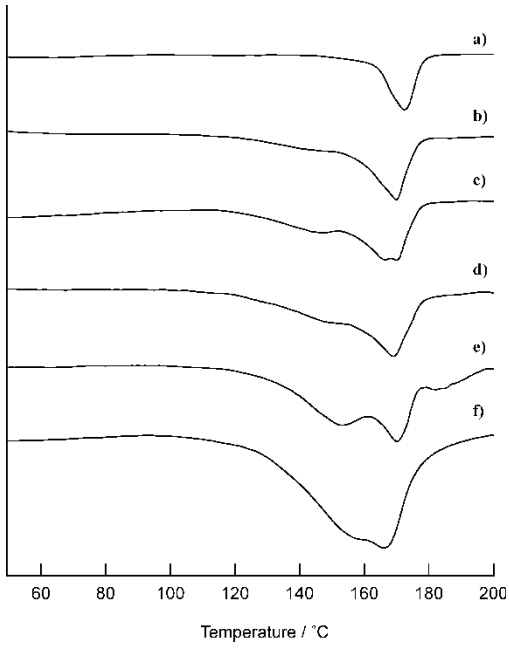

Figure 9. 1st heating process of DSC curves for $MgHPO_4$-PLLA system, $[Mg^{2+}]$ = a) 0, b) 0.394, c) 0.784, d) 1.20, e) 1.54 mmol g^{-1}, f) $MgHPO_4$.

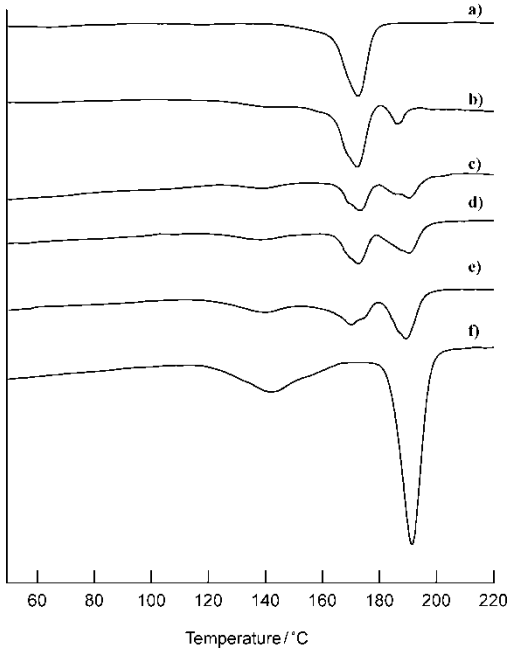

Figure 10. 1st heating process of DSC curves for $CaHPO_4$-PLLA system, $[Ca^{2+}]$ = a) 0, b) 0.463, c) 0.951, d) 1.43, e) 1.83 mmol g^{-1}, f) $CaHPO_4$.

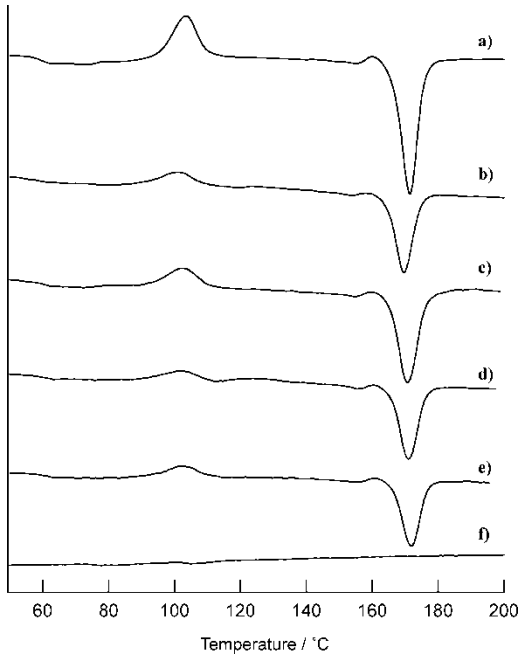

Figure 11. 2nd heating process of DSC curves for $MgHPO_4$-PLLA system, $[Mg^{2+}] = a)$ 0, b) 0.394, c) 0.784, d) 1.20, e) 1.54 mmol g^{-1}, f) $MgHPO_4$.

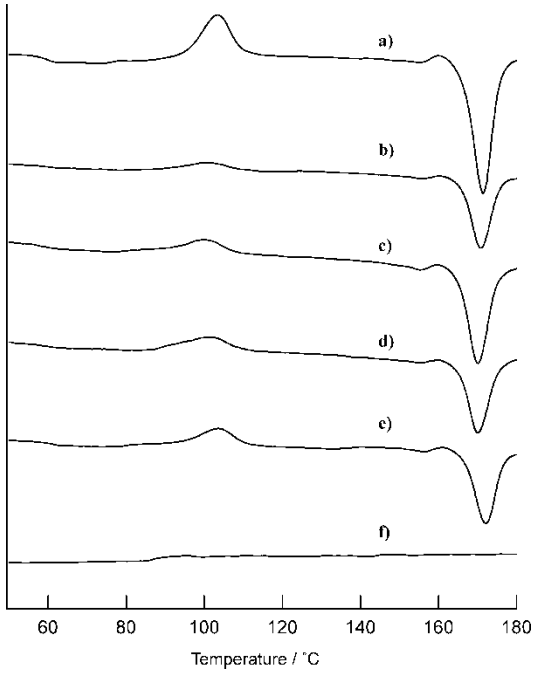

Figure 12. 2nd heating process of DSC curves for $CaHPO_4$-PLLA system, $[Ca^{2+}] = a)$ 0, b) 0.463, c) 0.951, d) 1.43, e) 1.83 mmol g^{-1}, f) $CaHPO_4$.

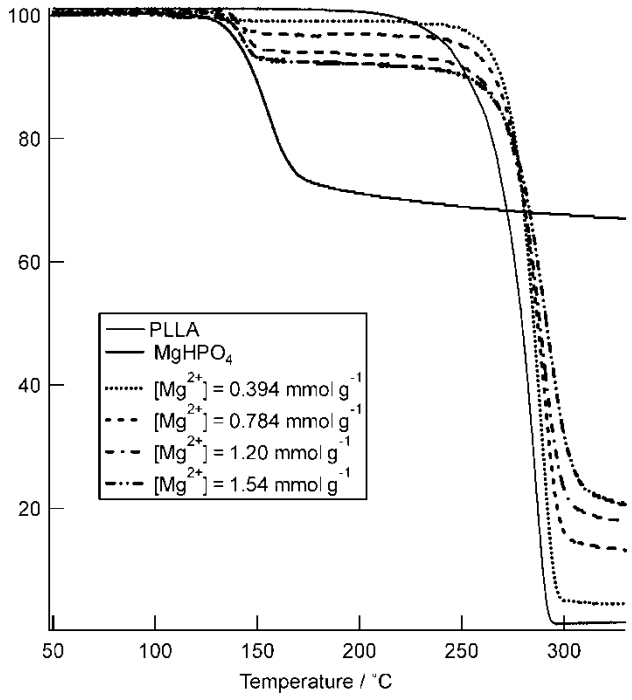

Figure 13. TGA curves for $MgHPO_4$-PLLA.

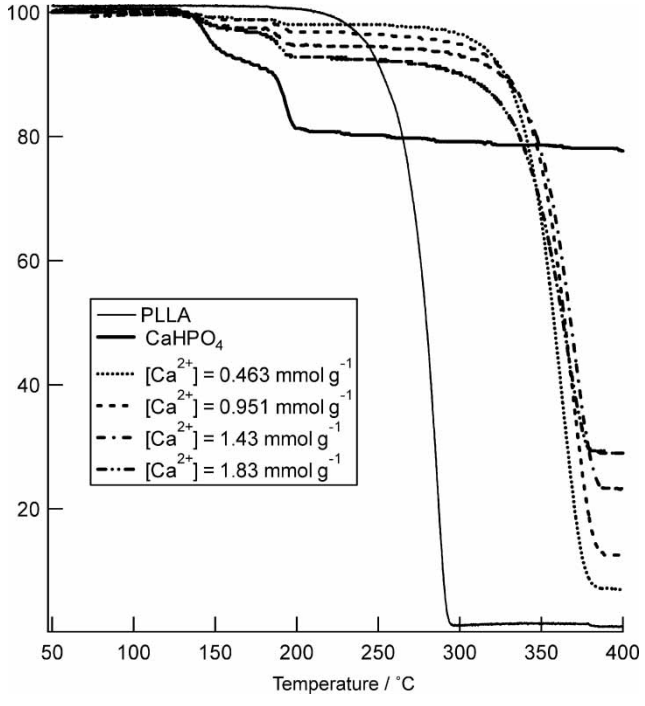

Figure 14. TGA curves for $MgHPO_4$-PLLA.

Table 2
Thermal properties of $MgHPO_4$-PLLA complex

$[Mg^{2+}]$/mmol g^{-1}	T_g/°C	T_c/°C	ΔH_c/J g^{-1}	T_m/°C	ΔH_m/J g^{-1}	T_d/°C
0	56 (1)	106 (0)	30 (3)	172 (0)	−36 (4)	253 (1)
0.394	57 (1)	101 (1)	10 (3)	170 (1)	−40 (6)	270 (2)
0.784	57 (1)	102 (1)	10 (4)	171 (1)	−40 (5)	270 (1)
1.20	57 (1)	102 (2)	9 (3)	171 (2)	−37 (5)	270 (1)
1.54	58 (1)	102 (1)	10 (5)	172 (2)	−38 (6)	270 (2)

In parenthesis: errors at decimal.

Table 3
Thermal properties of $CaHPO_4$-PLLA complex

$[Ca^{2+}]$/mmol g^{-1}	T_g/°C	T_c/°C	ΔH_c/J g^{-1}	T_m/°C	ΔH_m/J g^{-1}	T_d/°C
0	56 (1)	106 (0)	30 (3)	172 (0)	−36 (4)	253 (1)
0.463	58 (3)	101 (3)	10 (4)	171 (2)	−43 (5)	329 (1)
0.951	60 (2)	100 (2)	7 (3)	170 (1)	−36 (4)	330 (3)
1.43	62 (2)	102 (4)	8 (4)	170 (2)	−36 (4)	330 (1)
1.83	63 (3)	104 (5)	8 (6)	172 (3)	−29 (6)	331 (2)

In parenthesis: errors at decimal.

coordination number estimated to be 6.4, suggesting five or four phosphate oxygen coordinations to one or two PLLA oxygens. However, magnesium ion was not effective for forming such a structure due to the small ion radii. Calcium hydrogen phosphate was found to be more effective for increasing in T_g (about 5°C) than magnesium hydrogen phosphate as observed in DSC and TGA analyses. EXAFS studies indicated that the metal ion would be involved in a crosslinking point of the polymer chain leading to the complex formation such as metal-plla.

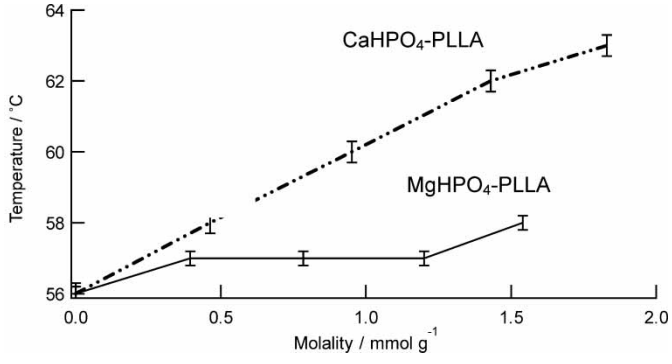

Figure 15. T_g dependence on metal ion.

Acknowledgements

We acknowledge Professor K. Ozutsumi (Department of Applied Chemistry, Faculty of Science and Engineering, Ritsumeikan University) for his helpful discussions for EXAFS measurements.

References

1. Weiler, A., Hoffmann, R.F.G., Stähelin, A.C., Helling, H.J., and Südkamp, N.P. (2000) Biodegradable Implants in Sports Medicine: The Biological Base. *Arthroscopy*, 16 (3): 305–321.
2. Nijsen, J.F.W., van het Schip, A.D., Hennink, W.E., Rook, D.W., van Rijk, P.P., and de Klerk, J.M.H. (2002) Advances in Nuclear Oncology: Microspheres for Internal Radionuclide Therapy of Liver Tumours. *Curr. Med. Chem.*, 9 (1): 73–82.
3. Nijsen, J.F.W., Zonnenberg, B.A., Woittiez, J.R.W., Rook, D.W., Swildens-van Woudenberg, I.A., van Rijk, P.P., and het Schip, A.D. (1999) Holmium-166 Poly Lactic Acid Microspheres Applicable for Intra-arterial Radionuclide Therapy of Hepatic Malignancies: Effects of Preparation and Neutron Activation Techniques. *Eur. J. Nucl. Med.*, 26 (7): 699–704.
4. Leeslag, J.W., Pennings, A.J., Bos, R.R.M., Rozema, F.R., and Boering, G. (1987) Resorbable Materials of Poly(L-Lactide). VI. Plates and Screws for Internal Fracture Fixation. *Biomaterials*, 8 (1): 70–73.
5. Vert, M., Charbot, F., Leray, J., and Christel, P. (1981) Bioresorbable Polyesters for Bone Surgery. *Makromol. Chem. Suppl.*, 5: 30–41.
6. Prasad, P.N., Mark, E., and Fai, T.J., eds. (1997) *Polymers and Other Advanced Materials*; Plenum Press: New York, 589.
7. Lostocco, M.R., Borzacchiello, A., and Huang, S.J. (1998) Binary and Ternary Poly(Lactic Acid)/Poly(ε-Caprolactone) Blends: The Effects of Oligo-ε-Caprolactones upon Mechanical Properties. *Macromol. Symp.*, 130: 151–160.
8. Hiljinen-Vainio, M., Varpomaa, P., Seppälä, J., and Törmälä, P. (1996) Modification of Poly(L-Lactides) by Blending: Mechanical and Hydrolytic Behavior. *Macromol. Chem. Phys.*, 197: 1503–1523.
9. Dobrzynski, P., Kasperczyk, J., Janeczek, H., and Bero, M. (2002) Synthesis of Biodegradable Glycolide/L-Lactide Copolymers Using Iron Compounds as Initiator. *Polymer*, 43 (9): 2595–2601.
10. Shirahama, H., Tanaka, A., Nagasawa, M., and Yasuda, H. (1999) Preparation and Enzymatic Degradation of Depsipeptide/Lactone/Lactide Terpolymers. *Kobunshi Ronbunshu*, 56 (9): 550–556.
11. Ferreira, B.M.P., Zavaglia, C.A.C., and Duek, E.A.R. (2001) Films of Poly(L-Lactic Acid)/Poly(Hydroxybutyrate-co-Hydroxyvalerate) Blends: *In Vitro* Degradation. *Mater. Res.*, 4 (1): 34–42.
12. Jianzhong, B.H. and Wang, S. (2003) Synthesis and Characterization of a Functionalized Biodegradable Copolymer: Poly(L-Lactide-*co*-*RS*-β-Malic Acid). *Polymer*, 44 (4): 989–994.
13. Fan, Y., Nishida, H., Hoshihara, S., Shirai, Y., Tokiwa, Y., and Endo, T. (2003) Pyrolysis Kinetics of Poly(L-Lactide) with Carboxyl and Calcium Salt End Structure. *Polym. Degrad. Stab.*, 79 (3): 547–562.
14. Lee, J.H., Park, T.G., Park, H.S., Lee, D.S., Lee, Y.K., Yoon, S.C., and Nam, J.D. (2003) Thermal and Mechanical Characteristics of Poly(L-Lactic Acid) Nanocomposite Scaffold. *Biomaterials*, 24 (16): 2773–2778.
15. Ignjatović, N., Tomić, S., Dakić, M., Miljković, M., Plavšić, M., and Usković, D. (1999) Synthesis and Properties of Hydroxyapatite/Poly-L-Lactide Composite Biomaterials. *Biomaterials*, 20 (9): 809–816.

16. Furukawa, T., Matsusue, Y., Yasunaga, T., Shikinami, Y., Okuno, M., and Nakamura, T. (2000) Biodegradation Behavior of Ultra-High-Strength Hydroxyapatite/Poly (L-Lactide) Composite Rods for Internal Fixation of Bone Fracture. *Biomaterials*, 21 (9): 889–898.
17. Mickiewicz, R.A. (2001) Master Thesis, Department of Material Science and Engineering, University of Massachusetts Institute of Technology.
18. Ueyama, N., Kozuki, H., Doi, M., Yamada, Y., Takahashi, K., Onoda, A., Okamura, T., and Yamamoto, H. (2001) Secure Binding of Alternately Amidated Poly(acrylate) to Crystalline Calcium Carbonate by NH·O Hydrogen Bond. *Macromol.*, 34 (8): 2607–2614.
19. Iucci, G., Infante, G., and Polzonetti, G. (2002) The Reaction Between Pt- and Pd-*cis* Di-Chloro Complexes and 4,4′-Diethynylbiphenyl: Synthesis and Characterisation of a 'Zigzag' Metal/Poly-yne Polymer. *Polymer*, 43 (3): 655–663.
20. Molochinikov, L.S., Kovalyova, E.G., Zagorodni, A.A., Muhammed, M., Sultanov, Y.M., and Ependier, A.A. (2003) Coordination of Cu(II) and Ni(II) in Polymers Imprinted so as to Optimize Amine Chelate Formation. *Polymer*, 44 (17): 4805–4815.
21. Nijsen, J.F.W., van Steenbergen, M.J., Kooijman, H., Talsma, H., Kroon-Batenburg, L.M.J., van de Weert, M., van Rijk, P.P., de Witte, A., van het Schip, A.D., and Hennink, W.E. (2001) Characterization of Poly(L-Lactic Acid) Microspheres Loaded with Holmium Acetylacetonate. *Biomaterials*, 22 (22): 3073–3081.
22. Shinno, K., Miyamoto, M., Kimura, Y., Hirai, Y., and Yoshitome, H. (1997) Solid-State Postpolymerization of L-Lactide Promoted by Crystallization of Product Polymer: An Effective Method Reduction of Remaining Monomer. *Macromol.*, 30 (21): 6438–6444.
23. Lee, P.A. and Pendry, J.B. (1975) Theory of the Extended X-ray Absorption Fine Structure. *Phys. Rev. B*, 11 (8): 2795–2811.
24. Dickens, B., Bowen, J.S., and Brown, W.E. (1971) A Refinement of the Crystal Structure of $CaHPO_4$ (Synthetic Monetite). *Acta Cryst. B*, 28: 798–806.
25. Curry, N.A. and Jones, D.W. (1971) Crystal Structure of Brushite, Calcium Hydrogen Orthophosphate Dihydrate: A Neutron-diffraction Investigation. *J. Chem. Soc. A*, 3725–3729.
26. McKale, A.D., Veal, B.W., Paulikas, A.P., Chan, S.K., and Knapp, G.S. (1988) Improved *ab Initio* Calculations of Amplitude and Phase Functions for Extended X-ray Absorption Fine Structure Spectroscopy. *J. Am. Chem. Soc.*, 110 (12): 3763–3768.
27. Shannon, R.D. (1976) Revised Effective Ionic Radii and Systematic Studies of Interatmic Distances in Halides and Chalcogenides. *Acta Cryst. A*, 32: 751–767.